

# Propane Dehydrogenation Over PtSn Catalysts Supported on ZnO-Modified MgAl<sub>2</sub>O<sub>4</sub>

Yaojie Wang · Yanmei Wang · Shurong Wang ·  
Xianzhi Guo · Shou-Min Zhang · Wei-Ping Huang ·  
Shihua Wu

Received: 11 June 2009 / Accepted: 28 July 2009 / Published online: 8 August 2009  
© Springer Science+Business Media, LLC 2009

**Abstract** Platinum and tin supported on ZnO-modified MgAl<sub>2</sub>O<sub>4</sub> constitutes a new and efficient catalyst for the dehydrogenation of propane. The structure of the catalyst has been studied by XRD, TEM, BET, TG, H<sub>2</sub>-TPR and H<sub>2</sub> chemisorption and catalytic properties for propane dehydrogenation have been tested on a microreactor. It has been shown that the catalyst is superior to conventional alumina-supported PtSn systems and PtSn/MgAl<sub>2</sub>O<sub>4</sub> in terms of lifetime stability, activity and propene selectivity. The characterization results of catalysts revealed that ZnO-modified catalysts can increase the Pt dispersion and enhance the interaction between metal and support, resulting in the increase of catalytic activity for propane dehydrogenation.

**Keywords** Pt · Sn · Al<sub>2</sub>O<sub>3</sub> · MgAl<sub>2</sub>O<sub>4</sub> · ZnO/MgAl<sub>2</sub>O<sub>4</sub> · Propane dehydrogenation

## 1 Introduction

Dehydrogenation of propane into propylene not only is an important way in the use of low-carbon alkane, but also makes up the increasing contradiction between supply and demand situation of propylene. Pt/Al<sub>2</sub>O<sub>3</sub> and PtSn/Al<sub>2</sub>O<sub>3</sub> catalyst have been widely used in hydrocarbon dehydrogenation [1–6], however, regarding the stability of the catalysts, the dehydrogenation performance of PtSn catalysts is still not satisfactory, several researches have been reported in

improving the catalytic stability of supported PtSn catalysts for low paraffin dehydrogenation by adding various promoters to PtSn/ $\gamma$ -Al<sub>2</sub>O<sub>3</sub> catalyst [7–11] and by using other supports instead of  $\gamma$ -Al<sub>2</sub>O<sub>3</sub> [12–17]. MgAl<sub>2</sub>O<sub>4</sub> and ZnAl<sub>2</sub>O<sub>4</sub> have characteristic of thermal stability, high mechanical strength, low surface acidity, which can be better adapted to low-carbon alkane dehydrogenation process of severe reaction conditions [18, 19]. There are many researches on the application of spinel as the supports of PtSn catalysts for butane dehydrogenation [20, 21], however, less attention has been paid to the catalysts supported on spinel for propane dehydrogenation. Aguilar-Ríos et al. [22] studied the propane dehydrogenation activity of Pt and Pt–Sn catalysts supported on magnesium aluminate, and found that the activity and propylene selectivity of the catalysts were low. Akporiaye et al. [16] reported a good dehydrogenation performance over PtSn/MgAl<sub>2</sub>O<sub>4</sub> catalyst which was obtained under the condition of 600 °C. Higher temperature is not conducive to industrialization application of catalysts.

This paper reports on a novel and efficient catalyst for propane dehydrogenation, which contains platinum promoted with tin supported on the mesoporous MgAl<sub>2</sub>O<sub>4</sub> modified by ZnO. The catalysts have good performance at low temperature. The catalysts were characterized with different analytical techniques (XRD, TEM, BET, TG analysis, chemical analysis). Their catalytic properties were evaluated in a microreactor.

## 2 Experimental Section

### 2.1 Preparation of MgAl<sub>2</sub>O<sub>4</sub>

MgAl<sub>2</sub>O<sub>4</sub> was prepared by the sol-gel method, magnesium nitrate [Mg(NO<sub>3</sub>)<sub>2</sub>·6H<sub>2</sub>O] and aluminum nitrate

Y. Wang · Y. Wang · S. Wang · X. Guo · S.-M. Zhang ·  
W.-P. Huang · S. Wu (✉)  
Department of Chemistry, Nankai University, 300071 Tianjin,  
China  
e-mail: wushh@nankai.edu.cn

[Al(NO<sub>3</sub>)<sub>3</sub>·9H<sub>2</sub>O] were dissolved in deionized water under magnetic stirring, the molar ratio of the two nitrates was determined according to the stoichiometric amount of MgAl<sub>2</sub>O<sub>4</sub>. Citric acid solution was prepared by adding citric acid (the amounts were 2 times of the metal ions in mole) into the deionized water. Citric acid solution was slowly added dropwise into the nitrate salt solution. The mixed solution was heated to 70–90 °C and stirred for 60 min with magnetic bar. The pH value of the solution was adjusted in the range of 2.0–3.0 by the addition of ammonia solution. The temperature was maintained at 70–90 °C until the gel was formed. The products were dried at 160 °C for 4 h in an oven and became honeycomb porous gels. The exergels were heat-treated at 800 °C for 4 h and finally MgAl<sub>2</sub>O<sub>4</sub> powders were obtained. All the chemicals used in the experiments are of analytical grade purity.

## 2.2 Preparation of Catalysts

Zinc oxide-modified MgAl<sub>2</sub>O<sub>4</sub> sample (ZnO 1.25 wt%) was prepared by impregnating the MgAl<sub>2</sub>O<sub>4</sub> powder sample into a zinc nitrate aqueous solution, dried in air at 120 °C for 8 h and calcined at 550 °C in air for 4 h. Catalyst was prepared by the sequence impregnating with equal aqueous solution of the Pt precursor (H<sub>2</sub>PtCl<sub>6</sub>) and SnCl<sub>2</sub> ethanol solution, Sn was first deposited. For comparison, Pt/MgAl<sub>2</sub>O<sub>4</sub>, PtZn/MgAl<sub>2</sub>O<sub>4</sub>, PtSn/γ-Al<sub>2</sub>O<sub>3</sub> (γ-Al<sub>2</sub>O<sub>3</sub>; BET 173 m<sup>2</sup>/g, Tianjin chemical industry institute) and PtSn/MgAl<sub>2</sub>O<sub>4</sub> were prepared at the same time. All samples (Pt 0.3%, Sn 1.2%) were dried at 120 °C for 8 h, and calcined in air at 550 °C for 4 h.

## 2.3 Propane Dehydrogenation

Catalysts were tested for the propane dehydrogenation reaction in a microreactor under reaction conditions of 0.1 MPa, 530 °C, C<sub>3</sub>H<sub>8</sub>/H<sub>2</sub> = 1/1 (molar ratio) and the total WHSV = 3.6 h<sup>-1</sup>. A sample (0.3 g), placed in a quartz fixed-bed reactor ( $L = 425$  mm,  $\Phi = 10$  mm), was previously heated to 530 °C under a flowing N<sub>2</sub> stream in a temperature programmed furnace. PtSn/ZnO/MgAl<sub>2</sub>O<sub>4</sub> catalyst was tested for the propane dehydrogenation at 490, 530 and 580 °C, respectively. The reaction products (C<sub>3</sub>H<sub>8</sub>, C<sub>3</sub>H<sub>6</sub>, CH<sub>4</sub>, C<sub>2</sub>H<sub>6</sub> and C<sub>2</sub>H<sub>4</sub>) were analyzed by an online gas chromatography (GC-7800) with FID detector and Porapak-Q packed column.

## 2.4 Regeneration by Coke Burning-off

Regeneration treatments were performed in the same quartz reactor as propane dehydrogenation loaded with 0.3 g of deactivated catalyst. The catalyst was heated in nitrogen from room temperature to 500 °C. Coke burning

was started by feeding the O<sub>2</sub>:N<sub>2</sub> mixture (5% O<sub>2</sub>) at 20 ml/min.

## 2.5 Characterizations

### 2.6 Powder X-ray Diffraction

The powder X-ray diffraction patterns of the MgAl<sub>2</sub>O<sub>4</sub> and ZnO/MgAl<sub>2</sub>O<sub>4</sub> samples were obtained on a rigaku D/max-2500 diffractometer with Cu-K $\alpha$  radiation at 40 kV and 100 mA in a scanning range of 3–80° ( $2\theta$ ). The diffraction peaks of the materials were compared with those of standard compounds reported in the JCPDS Date File.

### 2.6.1 Surface Area Measurements

N<sub>2</sub> adsorption–desorption isotherms were measured at –196 °C using a Quantachrome NOVA 2000e sorption analyzer. The samples were degassed at 200 °C for more than 6 h before analysis.

### 2.6.2 Transmission Electron Microscopy (TEM)

The measurements of morphology and metallic particle sizes of the catalysts were carried out in a Philips Tecnai G20 transmission electron microscope (TEM), operating at 200 kV.

### 2.6.3 Temperature-Programmed Reduction (TPR)

Temperature-programmed reduction (TPR) experiments were performed under the mixture of 5% H<sub>2</sub>/N<sub>2</sub> flowing (30 ml/min) over 20 mg of catalyst at a heating rate of 10 °C/min.

### 2.6.4 Thermo-Gravimetric (TG) Analysis

The amount of carbon deposited on the catalysts during propane dehydrogenation reaction was measured by using thermo-gravimetric (TG) analysis (ZRY-2P thermal analyzer). The catalyst samples (ca. 0.01 g) after reaction for 6 h were heated from room temperature to 800 °C in air with heating rate of 10 °C/min, and the amount of coke was calculated from TG curves.

### 2.6.5 Pulse Chemisorption of Hydrogen

Platinum dispersions were obtained by pulse H<sub>2</sub>-chemisorption. The experiments were carried out in the same setup as H<sub>2</sub>-TPR. Samples (0.2 g) were previously reduced under flowing pure H<sub>2</sub> (10 ml/min) at 500 °C for 2 h, then purged in N<sub>2</sub> at 540 °C for 2 h and cooled to 25 °C. The pulse size was 0.69 ml 5% (v/v) H<sub>2</sub> in N<sub>2</sub> mixture and the time between pulses was 3 min.

### 3 Results and Discussion

#### 3.1 Catalytic Properties

Table 1 shows the propane dehydrogenation of the PtSn/ZnO/MgAl<sub>2</sub>O<sub>4</sub> catalyst at 480, 530 and 550 °C, a deactivation parameter is defined as  $D$  ( $D = (X_0 - X_f)/X_0 \times 100$ ;  $X_0$  and  $X_f$  are the initial and final conversion) is used to characterize the activity decline.  $S_0$  and  $S_f$  represent the initial and final selectivity to propylene, respectively. The catalyst shows the highest initial conversion(43.3%) at 580 °C, but the value of deactivation parameter is 63.7%. when the reaction temperature is 530 °C, the catalyst exhibits the best performance than that of 480 and 580 °C.

Table 2 shows the catalytic performance of catalysts in the propane dehydrogenation reaction at 530 °C. Figures 1 and 2 shows propane conversion and propylene selectivity of the catalysts supported on different materials versus time on stream. The initial conversions of propane catalyzed by Pt/MgAl<sub>2</sub>O<sub>4</sub>, PtZn/MgAl<sub>2</sub>O<sub>4</sub>, PtSn/ $\gamma$ -Al<sub>2</sub>O<sub>3</sub>, PtSn/MgAl<sub>2</sub>O<sub>4</sub> and PtSn/ZnO/MgAl<sub>2</sub>O<sub>4</sub> are 23.4, 27.5, 31.6, 28.3 and 39.9%. The values of  $D$  for Pt/MgAl<sub>2</sub>O<sub>4</sub>, PtZn/MgAl<sub>2</sub>O<sub>4</sub>, PtSn/ $\gamma$ -Al<sub>2</sub>O<sub>3</sub>, PtSn/MgAl<sub>2</sub>O<sub>4</sub> and PtSn/ZnO/MgAl<sub>2</sub>O<sub>4</sub> are 74.7, 63.6, 45.4, 57.1 and 40.9%. Addition of ZnO to Pt/MgAl<sub>2</sub>O<sub>4</sub> induces the increase in conversion of propane and selectivity towards propylene. PtSn/ZnO/MgAl<sub>2</sub>O<sub>4</sub> exhibits the highest initial activity (39.9%) and the lowest deactivation value (40.9%). PtSn/MgAl<sub>2</sub>O<sub>4</sub> and PtSn/ZnO/MgAl<sub>2</sub>O<sub>4</sub> show the same propylene selectivity for propane dehydrogenation while Pt/MgAl<sub>2</sub>O<sub>4</sub> shows lower propylene selectivity than the above catalysts. The results indicated that modification of MgAl<sub>2</sub>O<sub>4</sub> by ZnO can enhance the catalytic activity and stability of PtSn/MgAl<sub>2</sub>O<sub>4</sub> catalysts. Zn is an electropositive element which was used as a promoter in Pt based catalysts for dehydrogenation of propane, the addition of the electropositive metal to platinum catalysts leads to increased activity, improved product selectivity and catalyst lifetime [15].

The initial conversion of Pt/MgAl<sub>2</sub>O<sub>4</sub> is 23.4% and the deactivation value is 74.7%. Addition of Sn to Pt/MgAl<sub>2</sub>O<sub>4</sub> results in an increase in conversion of propane (28.3%), selectivity towards propylene (99.6%) and the stability of catalysts. Compared the performance of PtZn/MgAl<sub>2</sub>O<sub>4</sub> with PtSn/ZnO/MgAl<sub>2</sub>O<sub>4</sub>, the same fact that Sn plays an

**Table 2** The activity, selectivity and deactivation of dehydrogenation on different catalysts

Catalyst	$X_0$ (%)	$X_f$ (%)	$(X_0 - X_f)/X_0 \times 100$ (%)	$S_0$	$S_f$
Pt/MgAl <sub>2</sub> O <sub>4</sub>	23.4	5.9	74.7	92.4	98.3
PtZn/MgAl <sub>2</sub> O <sub>4</sub>	27.5	10	63.6	93.8	99
PtSn/MgAl <sub>2</sub> O <sub>4</sub>	28.3	12.1	57.1	99.4	99.5
PtSn/ $\gamma$ -Al <sub>2</sub> O <sub>3</sub>	31.6	17.3	45.4	90.4	99.2
PtSn/ZnO/MgAl <sub>2</sub> O <sub>4</sub>	39.9	23.6	40.9	98.4	99.6

Reaction temperature: 530 °C

important role on the performance of Pt catalysts can be found. Many studies have extensively been investigated on the role of Sn in PtSn catalysts [1, 13, 23]. The role of Sn in PtSn catalysts is geometric effect and electronic effect [24], since tin can decrease the size of platinum ensembles and modify the electronic density of Pt. Addition of Sn to Pt/MgAl<sub>2</sub>O<sub>4</sub> and Pt/ZnO/MgAl<sub>2</sub>O<sub>4</sub> promotes desired dehydrogenation reactions, inhibits coking reactions and leads to high dehydrogenation performance of PtSn/ZnO/MgAl<sub>2</sub>O<sub>4</sub>.

Table 3 shows the particle size of the catalysts determined by H<sub>2</sub>-chemisorption, the particle size of the catalysts Pt/MgAl<sub>2</sub>O<sub>4</sub>, PtZn/MgAl<sub>2</sub>O<sub>4</sub>, PtSn/MgAl<sub>2</sub>O<sub>4</sub>, PtSn/ $\gamma$ -Al<sub>2</sub>O<sub>3</sub> and PtSn/ZnO/MgAl<sub>2</sub>O<sub>4</sub> are 6.3 nm, 3.9 nm, 3.2 nm, 2.7 nm and 2.4 nm. PtSn/ZnO/MgAl<sub>2</sub>O<sub>4</sub> has the smallest particle size but the highest catalytic performance. It was shown that the catalysts with small particle size show high performance on dehydrogenation of propane. Santhosh Kumar et al. [25] studied the dehydrogenation of propane (DHP) over monometallic Pt-SBA-15 catalysts and revealed that the catalysts with smaller particles show more active and less selective than that with larger particles. Addition of Sn and Zn can increase the dispersion and decrease the size of platinum ensembles, hydrogenolysis and coking reactions that require large platinum ensembles are reduced.

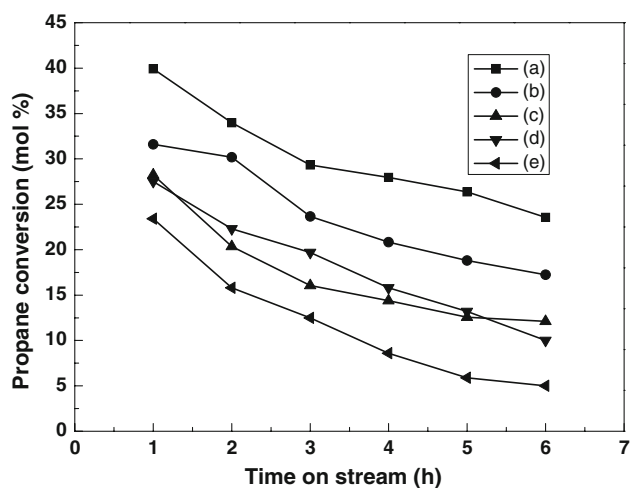
#### 3.2 Characterizations of Catalyst

Figure 3 shows the XRD patterns of the MgAl<sub>2</sub>O<sub>4</sub>, ZnO/MgAl<sub>2</sub>O<sub>4</sub>, PtSn/MgAl<sub>2</sub>O<sub>4</sub>, PtSn/ZnO/MgAl<sub>2</sub>O<sub>4</sub>,  $\gamma$ -Al<sub>2</sub>O<sub>3</sub>

**Table 1** Effect the temperature on the activity, selectivity and deactivation of dehydrogenation

PtSn/ZnO/MgAl <sub>2</sub> O <sub>4</sub>	$X_0$ (%)	$X_f$ (%)	$(X_0 - X_f)/X_0 \times 100$ (%)	$S_0$ (%)	$S_f$ (%)
480 °C	24.5	11	55.1	95.1	99.7
530 °C	39.3	23.6	39.9	98.4	99.6
580 °C	43.3	15.7	63.7	97.3	97.8

Deactivation parameter defined as  $[(X_0 - X_f)/X_0 \times 100]$ ;  $X_0$  is initial conversion the  $X_f$  is the final conversion, initial selectivity ( $S_0$ ) and final selectivity ( $S_f$ ) to propylene



**Fig. 1** The propane conversion of catalysts supported on different materials: *a* PtSn/ZnO/MgAl<sub>2</sub>O<sub>4</sub>, *b* PtSn/ $\gamma$ -Al<sub>2</sub>O<sub>3</sub>, and *c* PtSn/MgAl<sub>2</sub>O<sub>4</sub>, *d* Pt/ZnO/MgAl<sub>2</sub>O<sub>4</sub>, *e* Pt/MgAl<sub>2</sub>O<sub>4</sub>

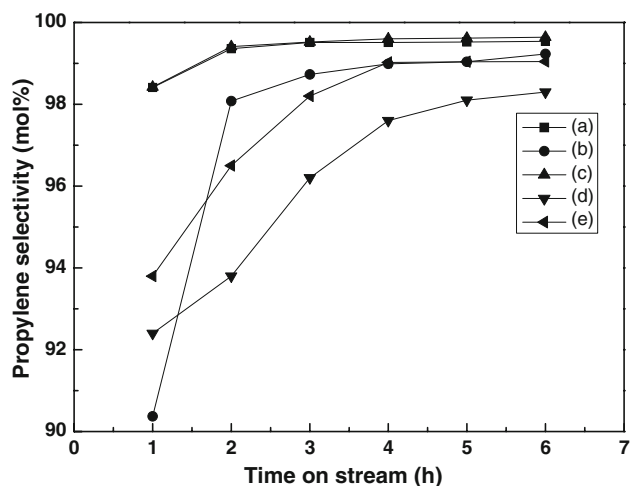


**Fig. 2** The propylene selectivity over catalysts supported on different materials: *a* PtSn/MgAl<sub>2</sub>O<sub>4</sub>, *b* PtSn/ $\gamma$ -Al<sub>2</sub>O<sub>3</sub>, *c* PtSn/ZnO/MgAl<sub>2</sub>O<sub>4</sub>, *d* Pt/MgAl<sub>2</sub>O<sub>4</sub>, *e* Pt/ZnO/MgAl<sub>2</sub>O<sub>4</sub>

and PtSn/ $\gamma$ -Al<sub>2</sub>O<sub>3</sub> samples. By comparing the diffractograms of Fig. 3a [shows the presence of the MgAl<sub>2</sub>O<sub>4</sub> spinel (JCPDS 73-2210)] and Fig 3b (shows the patterns of the ZnO/MgAl<sub>2</sub>O<sub>4</sub>), it is found that the peaks are the same as MgAl<sub>2</sub>O<sub>4</sub> spinel and there is no evidence of crystalline ZnO, which shows that ZnO-modifying doesn't change the structure of MgAl<sub>2</sub>O<sub>4</sub>. Fig 3c, d show the similar peaks as MgAl<sub>2</sub>O<sub>4</sub>. Fig 3e shows the patterns of the  $\gamma$ -Al<sub>2</sub>O<sub>3</sub> (JCPDS10-425), Fig 3f shows the same peaks as  $\gamma$ -Al<sub>2</sub>O<sub>3</sub>. No catalysts show evidence of Pt and Sn, due to low concentration of Pt and Sn or their small crystallite size [8]. Figure 4 shows the nitrogen adsorption–desorption isotherms of PtSn/ $\gamma$ -Al<sub>2</sub>O<sub>3</sub>, PtSn/MgAl<sub>2</sub>O<sub>4</sub> and PtSn/ZnO/MgAl<sub>2</sub>O<sub>4</sub> samples, the three

**Table 3** Particle size of catalysts

Catalyst	Particle size (nm)		
	TEM	XRD <sup>a</sup>	H <sub>2</sub> -Chemisorption <sup>b</sup>
Pt/MgAl <sub>2</sub> O <sub>4</sub>			6.3
PtZn/MgAl <sub>2</sub> O <sub>4</sub>			3.9
PtSn/MgAl <sub>2</sub> O <sub>4</sub>	6–8		3.2
PtSn/ $\gamma$ -Al <sub>2</sub> O <sub>3</sub>	5–7		2.7
PtSn/ZnO/MgAl <sub>2</sub> O <sub>4</sub>	6–8		2.4

<sup>a</sup> No diffraction peaks of Pt and Sn

<sup>b</sup> Determined by  $d \text{ (nm)} = 1.13/D$  ( $D$  dispersion)

catalysts exhibited type IV adsorption–desorption isotherms, which is characteristic of mesoporous materials. Figure 5 shows the pore size distribution curves of PtSn/Al<sub>2</sub>O<sub>3</sub>, PtSn/MgAl<sub>2</sub>O<sub>4</sub> and PtSn/ZnO/MgAl<sub>2</sub>O<sub>4</sub> samples. It can be seen that the most possible pore diameter of PtSn/MgAl<sub>2</sub>O<sub>4</sub> is 2.5 nm and 11.5 nm (curve a), while the PtSn/ZnO/MgAl<sub>2</sub>O<sub>4</sub> sample has two kinds of pore with the most possible diameter of 2 and 8 nm (curve b), which indicates the pore size distribution of PtSn/MgAl<sub>2</sub>O<sub>4</sub> was shifted to more pores of smaller diameters after loading of ZnO, and it seems reasonable to consider that ZnO may reside inside the pores. The PtSn/Al<sub>2</sub>O<sub>3</sub> sample used in this work has pores with diameter of 7.05 nm (curve b). Textural properties of the samples were measured by nitrogen adsorption–desorption isotherms and shown in Table 4. PtSn/Al<sub>2</sub>O<sub>3</sub> has area of 174.59 m<sup>2</sup>/g and PtSn/MgAl<sub>2</sub>O<sub>4</sub> has surface area of 138.4 m<sup>2</sup>/g, while PtSn/ZnO/MgAl<sub>2</sub>O<sub>4</sub> shows surface area of 174.7 m<sup>2</sup>/g. The modification of PtSn/MgAl<sub>2</sub>O<sub>4</sub> by ZnO leads to an increase in the surface area. The TEM results shown in Figure 6 indicate that the metal particle sizes of PtSn/MgAl<sub>2</sub>O<sub>4</sub> and PtSn/ZnO/MgAl<sub>2</sub>O<sub>4</sub> catalysts are almost the same (ca. 6–8 nm), the particle size of PtSn/ $\gamma$ -Al<sub>2</sub>O<sub>3</sub> is about 5–7 nm. The partial size of spent PtSn/ $\gamma$ -Al<sub>2</sub>O<sub>3</sub> increases obviously and the coke is deposited on the surface of the catalyst.

### 3.3 Surface Properties of Catalysts

#### 3.3.1 Pt Dispersion

Table 5 shows the platinum dispersion of catalysts. Platinum dispersion was calculated from hydrogen pulse chemisorption on the basis of H:Pt = 1 [26]. ZnO doped Pt/MgAl<sub>2</sub>O<sub>4</sub> and PtSn/MgAl<sub>2</sub>O<sub>4</sub> catalysts lead to an obvious increase in platinum dispersion which is also influenced by the addition of Sn. The existence of ZnO in Pt and PtSn catalysts can promote the activity and stability of dehydrogenation, it can be partly attributed to the increase in platinum dispersion. Studies have shown that the active site for propane dehydrogenation is the single platinum

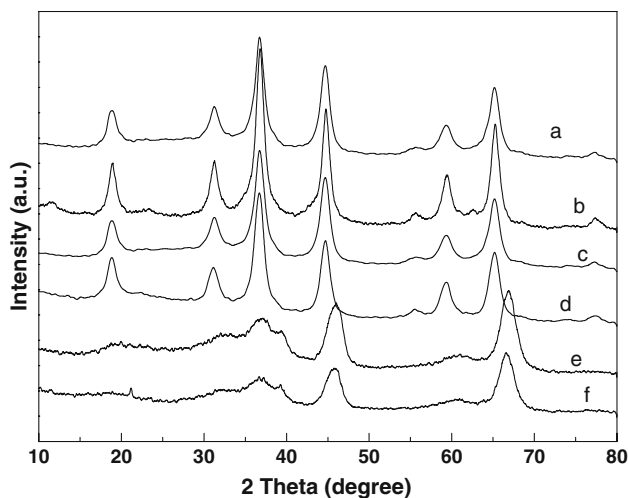


**Fig. 3** XRD patterns: *a*  $\text{MgAl}_2\text{O}_4$ , *b*  $\text{ZnO/MgAl}_2\text{O}_4$ , *c*  $\text{PtSn/MgAl}_2\text{O}_4$ , *d*  $\text{PtSn/ZnO/MgAl}_2\text{O}_4$ , *e*  $\gamma\text{-Al}_2\text{O}_3$ , *f*  $\text{PtSn}/\gamma\text{-Al}_2\text{O}_3$

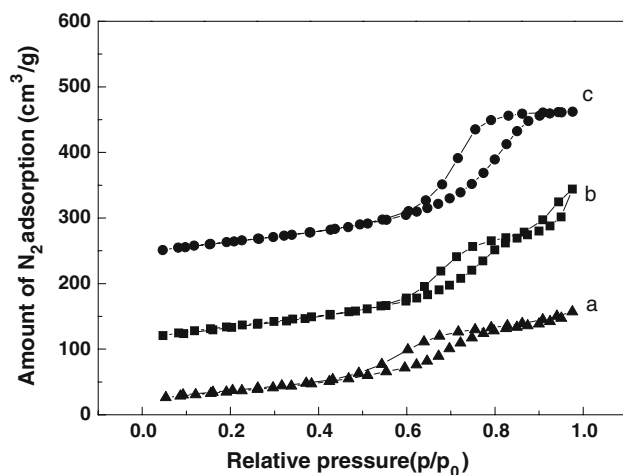


**Fig. 4** Nitrogen adsorption–desorption isotherms of different samples: *a*  $\text{PtSn/MgAl}_2\text{O}_4$ , *b*  $\text{PtSn/ZnO/MgAl}_2\text{O}_4$ , *c*  $\text{PtSn}/\gamma\text{-Al}_2\text{O}_3$

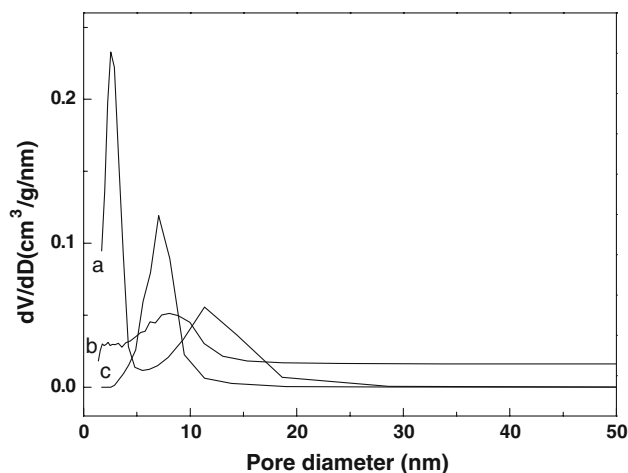


**Fig. 5** Pore size distribution curve of the different samples: *a*  $\text{PtSn/MgAl}_2\text{O}_4$ , *b*  $\text{PtSn/ZnO/MgAl}_2\text{O}_4$ , *c*  $\text{PtSn}/\gamma\text{-Al}_2\text{O}_3$

atom, while hydrogenolysis and coke reactions require the large platinum particles [27]. Furthermore, zinc can reduce the size of the platinum particles as the role of tin in PtSn catalyst and suppress the side reactions which need large platinum ensembles.

### 3.3.2 TPR Analysis

Figure 7 shows the TPR profiles of  $\text{Pt/MgAl}_2\text{O}_4$ ,  $\text{PtSn/MgAl}_2\text{O}_4$ ,  $\text{PtSn}/\gamma\text{-Al}_2\text{O}_3$ ,  $\text{PtSn/ZnO/MgAl}_2\text{O}_4$  and  $\text{PtSn}/\gamma\text{-Al}_2\text{O}_3$  catalysts respectively. The TPR profile of  $\text{PtSn}/\gamma\text{-Al}_2\text{O}_3$  sample is composed of three  $\text{H}_2$  consumption peaks (curve e). There are two low temperature peaks: the first one around 250 °C and the second one around 450 °C can be assigned to the co-reduction of Pt and Sn [1]. The third one around 680 °C can be assigned to reduction of  $\text{Al}^{3+}$  ions in alumina surface layers [8, 28]. All the catalysts supported on the  $\text{MgAl}_2\text{O}_4$  show two reduction peaks at about 600 and 750 °C. The origin of the two peaks is not clearly known, but it is speculated that it is linked with the reduction of OH groups or aluminum ions on the surface of  $\text{MgAl}_2\text{O}_4$ . Over the  $\text{Pt/MgAl}_2\text{O}_4$  (curve a), two reduction peaks appear, one near 230 °C and another around 470 °C. Two types of Pt oxides are considered in literatures [29–31]. The former is reduced at low temperatures due to weak interaction with the support, the latter requires higher temperatures on account of strong interaction. Therefore, we can associate the hydrogen consumption peaks at 230 and 470 °C with the reduction of two kinds of platinum. In the case of the  $\text{PtSn/MgAl}_2\text{O}_4$  (curve b), two reduction peaks are present, one at 260 °C, and the other at 430 °C. These two reduction peaks can be related to the co-reduction of platinum and tin particles. Pt assists the reduction of  $\text{SnO}_2$ , as reported by other groups [32, 33]. For the  $\text{PtZn/MgAl}_2\text{O}_4$  catalyst (curve c), the reduction peaks show similarities to those over  $\text{Pt/MgAl}_2\text{O}_4$ . Over  $\text{Pt/ZnO}$  sample, ZnO can be reduced to metallic Zn and lead to the formation of PtZn alloy even at low reduction temperatures (200 °C) [34]. It implies that there is a possibility of existence of PtZn alloy in  $\text{PtZn/MgAl}_2\text{O}_4$  catalyst. For  $\text{PtSn/ZnO/MgAl}_2\text{O}_4$  catalyst (curve d), only one large reduction peak appears around 400 °C, which can not be assigned to reduction of certain species. It is reasonable to assign this peak to the conjunct reduction of platinum, tin and zinc species. The presence of zinc changed the reduction property of the PtSn catalyst. The TPR profile suggests that strong interactions between zinc, tin and platinum three components may take place.

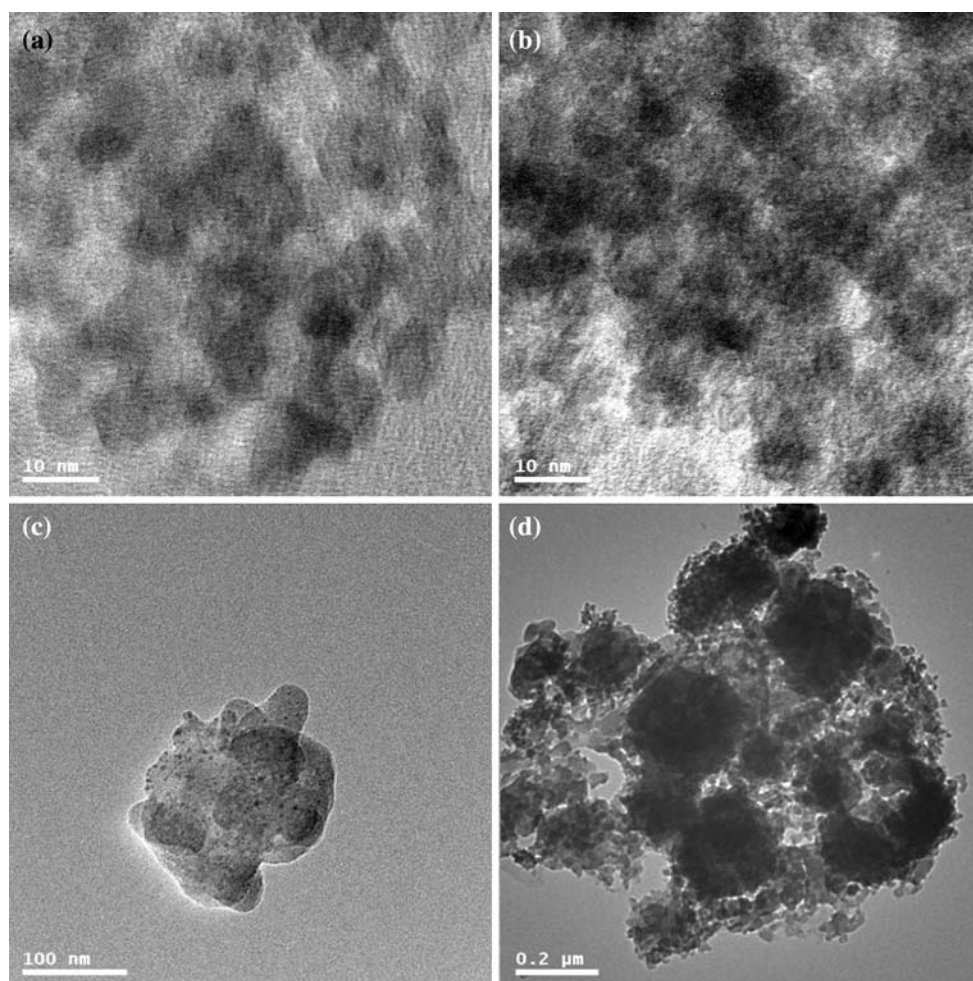
### 3.3.3 Analysis of Coke

The amount of coke deposited on the catalysts after dehydrogenation reaction for 6 h was measured by using



**Table 4** Textural properties of different samples

Sample	BJH average pore diameter(nm)	BET surface area (m <sup>2</sup> /g)	Total pore volume (cm <sup>3</sup> /g)
PtSn/MgAl <sub>2</sub> O <sub>4</sub>	4.3	138.4	0.822
PtSn/ZnO/MgAl <sub>2</sub> O <sub>4</sub>	9.1	174.7	0.404
PtSn/ $\gamma$ -Al <sub>2</sub> O <sub>3</sub>	7	174.6	0.384

**Fig. 6** TEM images of the different catalysts: **a** PtSn/MgAl<sub>2</sub>O<sub>4</sub>, **b** PtSn/ZnO/MgAl<sub>2</sub>O<sub>4</sub>, **c** PtSn/ $\gamma$ -Al<sub>2</sub>O<sub>3</sub>, **d** spent PtSn/ $\gamma$ -Al<sub>2</sub>O<sub>3</sub>**Table 5** Dispersion of catalysts

Catalyst	Dispersion
Pt/MgAl <sub>2</sub> O <sub>4</sub>	0.18
PtZn/MgAl <sub>2</sub> O <sub>4</sub>	0.29
PtSn/MgAl <sub>2</sub> O <sub>4</sub>	0.35
PtSn/ $\gamma$ -Al <sub>2</sub> O <sub>3</sub>	0.42
PtSn/ZnO/MgAl <sub>2</sub> O <sub>4</sub>	0.48

thermo-gravimetric (TG) analysis. As shown in Table 6, the amount of coke on PtSn/ $\gamma$ -Al<sub>2</sub>O<sub>3</sub>, PtSn/MgAl<sub>2</sub>O<sub>4</sub>, PtSn/ZnO/MgAl<sub>2</sub>O<sub>4</sub>, Pt/MgAl<sub>2</sub>O<sub>4</sub> and PtZn/MgAl<sub>2</sub>O<sub>4</sub> is 13.2%, 7.73, 7.51, 8.79 and 7.63%, respectively. The lowest

amount of coke is observed over the PtSn/ZnO/MgAl<sub>2</sub>O<sub>4</sub> catalyst and the highest amount of coke appears over the PtSn/ $\gamma$ -Al<sub>2</sub>O<sub>3</sub> catalyst. Santhosh Kumar et al. [25] reported that smaller particles are more active for propane conversion and coke formation. If we correlate the coke deposited to the particle size, we can find that there exists a mismatch or disproportion between them. Factors including support, surface acidity of catalysts, addition of promoter and interaction between metal and support that affect the formation of coke are complex, therefore, it is necessary to further study the effect on coke formation. Addition of Sn to Pt/MgAl<sub>2</sub>O<sub>4</sub> catalyst is to promote desired dehydrogenation reactions and inhibit coking reactions [27]. The effect of tin can be explained in geometric effect and electronic

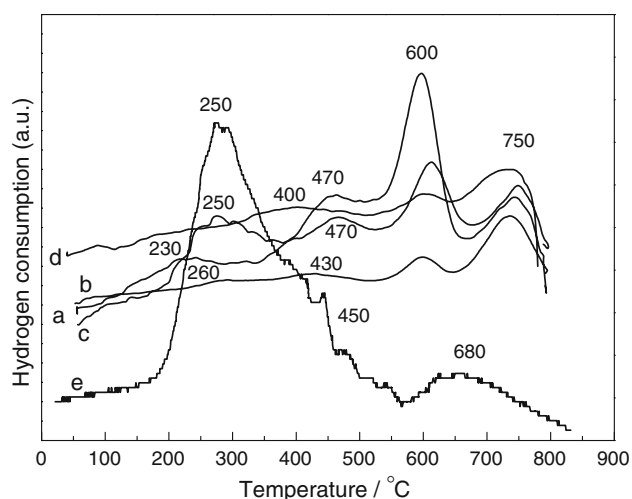


**Fig. 7** Temperature-programmed reduction (TPR) profiles of different samples: *a* Pt/MgAl<sub>2</sub>O<sub>4</sub>, *b* PtSn/MgAl<sub>2</sub>O<sub>4</sub>, *c* PtZn/MgAl<sub>2</sub>O<sub>4</sub>, *d* PtSn/ZnO/MgAl<sub>2</sub>O<sub>4</sub>, *e* PtSn/γ-Al<sub>2</sub>O<sub>3</sub>

**Table 6** The amount of coke deposits on different PtSn catalysts (after reaction for 6 h)

Catalyst	PtSn/ γ-Al <sub>2</sub> O <sub>3</sub>	PtSn/ MgAl <sub>2</sub> O <sub>4</sub>	PtSn/ZnO/ MgAl <sub>2</sub> O <sub>4</sub>	Pt/MgAl <sub>2</sub> O <sub>4</sub>	PtZn/ MgAl <sub>2</sub> O <sub>4</sub>
Coke amount (wt%)	13.2	7.73	7.51	8.79	7.63

effect [24]. Hydrogenolysis and coking reactions require large platinum ensembles, addition of Sn decreases the size of platinum ensembles. The presence of Sn brings about an increase in the electronic density of the platinum metal phase, which will weaken the strength of the Pt-(C=C) bond and repulse coke precursors. The presence of zinc can cause similar effects to Sn for the modification of Pt catalysts in dehydrogenation processes (Table 7).

Davis et al. [35] gave a surface figure of metal catalyst in the reaction, deposition carbon is formed on the surface of the catalyst, there are reactant and product molecules adsorbed on the catalyst surface. If the desorption is not successful, then eventually carbon deposition will be formed. Catalyst deactivation caused by carbon deposition has two possibilities: carbon deposits on the surface of active metal and carbon deposition blocks the pore of catalyst. This will reduce catalyst active site and cause the loss of some activity. Some researches have been done on deposition carbon of the catalyst surface about supported Pt catalysts [36, 37]. From TEM (Fig. 7d) of the spent catalyst, it can be seen that Pt particles increase markedly. Sintering of the active component and carbon deposition are two important factors of catalyst deactivation.

**Table 7** Effect of regeneration on the activity and deactivation of dehydrogenation

Catalyst	X <sub>0</sub> (%)	X <sub>f</sub> (%)	(X <sub>0</sub> - X <sub>f</sub> )/ X <sub>0</sub> × 100 (%)
PtSn/ZnO/MgAl <sub>2</sub> O <sub>4</sub>	39.9	23.6	40.9
The first regeneration	35.1	20.8	45.3
The second regeneration	31.9	15.4	51.7
The third regeneration	27.3	10.1	63

### 3.3.4 Regeneration Test

Figure 5 shows propane conversion of the fresh PtSn/ZnO/MgAl<sub>2</sub>O<sub>4</sub>, the first cycle regeneration of deactivated PtSn/ZnO/MgAl<sub>2</sub>O<sub>4</sub>, the second cycle regeneration and the third cycle regeneration.

The initial and final conversions of PtSn/ZnO/MgAl<sub>2</sub>O<sub>4</sub> decrease with the increase of regeneration cycle (initial conversion: from 39.9 to 27.3%, the final conversion: from 23.6 to 10.1%). The value of D increases from 40.9 to 63, which shows that the activity and stability of PtSn/ZnO/MgAl<sub>2</sub>O<sub>4</sub> decline with the regeneration cycle. The catalysts show the same propylene selectivity for propane dehydrogenation after regeneration (not shown). Recycle regeneration will give rise to two major poisoning processes [28]: the damage of the surface structure and the sintering of active component, which lead to deactivation of the catalysts.

## 4 Conclusions

The PtSn catalyst supported on ZnO-modified MgAl<sub>2</sub>O<sub>4</sub> (ZnO/MgAl<sub>2</sub>O<sub>4</sub>) exhibits higher activity and higher stability than the PtSn/MgAl<sub>2</sub>O<sub>4</sub> catalyst and conventional PtSn/γ-Al<sub>2</sub>O<sub>3</sub> catalyst for propane dehydrogenation. The higher catalytic activity and stability of PtSn/ZnO/MgAl<sub>2</sub>O<sub>4</sub> catalyst can be due to the presence of ZnO, which increases the Pt dispersion, reduces the metal particle size and enhances the interaction between the metal and the support.

**Acknowledgments** This work was supported by the National Natural Science Foundation of China (Nos. 20771061 and 20871071), 973 program (2005CB623607), and the Applied Basic Research Programs of Science and Technology Commission Foundation of Tianjin (Nos. 08JCYBJC00100 and 09JCYBJC03600).

## References

- Bariás OA, Holmen A, Blekkan EA (1996) *J Catal* 158:1
- Rebo HP, Blekkan EA, Holmen A (1999) *Stud Surf Sci Catal* 126:333

3. Rombi E, Cutrufello MG, Solinas V, Rosso SD, Ferraris G, Pistone A (2003) *Appl Catal A* 251:255
4. Rodriguez D, Sanchez J, Arteaga G (2005) *J Mol Catal A Chem* 228:309
5. Li RX, Wong NB, Tin KC (1998) *Catal Lett* 50:219
6. de Miguel SR, Jablonski EL, Castro AA (2000) *J Chem Tech Biotech* 5:596
7. Yu CL, Ge QG, Xu HY, Li WZ (2006) *Appl Catal A* 315:58
8. Yu CL, Xu HY, Ge QG, Li WZ (2007) *J Mol Catal A Chem* 266:80
9. Casella ML, Siri GJ, Santori GF et al (2000) *Langmuir* 16:5639
10. Del Angel G, Bonilla A, Peña Y, Navarrete J, Fierro JLG, Acosta DR (2003) *J Catal* 219:63
11. Siri GJ, Bertolini GR, Casella ML, Ferretti OA (2005) *Mater Lett* 59:2319
12. Waku T, Biscardi JA, Iglesia E (2004) *J Catal* 222:481
13. Stagg SM, Querini CA, Alvarez WE, Resasco DE (1997) *J Catal* 168:75
14. Zhang YW, Zhou YM, Qiu AD, Wang Y, Xu Y, Wu PC (2006) *Catal Commun* 7:860
15. Cola PLD, Gläser R, Weitkamp J (2006) *Appl Catal A* 306:85
16. Akporiaye D, Jensen SF, Olsbye U, Rohr F, Rytter E, Rønnekleiv M, Spjelkavik AI (2001) *Ind Eng Chem Res* 40:4741
17. Santhosh Kumar M, Chen D, Holmen A, Walmsley JC (2009) *Catal Today* 142:17
18. Padró CL, de Miguel SR, Castro AA, Scelza OA (1997) *Stud Surf Sci Catal* 111:191
19. Bosch P, Valenzuela MA, Zapata B, Acosta D, Aguilar-Ríos G, Maldonado C, Shifter I (1994) *J Mol Catal* 93:67
20. Bocanegra SA, Guerrero-Ruiz A, de Miguel SR (2004) *Appl Catal A* 277:11
21. Bocanegra Sonia A, de Miguel SR, Castro AA, Scelza OA (2004) *Catal Lett* 96:3
22. Aguilar-Ríos G, Salas P, Valenzuela MA, Armendáriz H, Wang JA, Salmones J (1999) *Catal Lett* 60:21
23. Schmal FBPM, Vannice MA (1996) *J Catal* 160:106
24. Llorca J, Homs N, Leon J, Sales J, Fierro JLG, Ramirez P (1999) *Appl Catal A* 189:77
25. Santhosh Kumar M, Chen De, Walmsley JC, Holmen Anders (2008) *Catal Commun* 9:747
26. Hu LJ, Boateng KA, Hill JM (2006) *J Mol Catal A* 259:51
27. Kogan SB, Schramm H, Herskowitz M (2001) *Appl Catal A* 208:185
28. Fan YN, Xu ZS, Zang ZL, Lin LW (1991) *Stud Surf Sci Catal* 68:683
29. Merlen M, Beccat P, Bertolini JC, Delichere P, Zanier N, Didillon B (1996) *J Catal* 159:178
30. Liezke H, Lietz G, Spindler H, Volter J (1983) *J Catal* 81:8
31. Armendáriz H, Guzmán A, Toledo JA, Llanos ME, Vázquez A, Aguilar-Ríos G (2001) *Appl Catal A Gen* 211:75
32. Liersk H, Volter J (1984) *J Catal* 90:96
33. De Miguel SR, Baronetti GT, Castro AA, Scelza OA (1988) *Appl Catal* 45:61
34. Consonni M, Jokic D, Murzin DY, Touroude R (1999) *J Catal* 188:165
35. Davis SM, Zaera F, Somorjai GA (1982) *J Catal* 77:439
36. Li CL, Novaroa O, Bokhimi X, Munoz E, Boldú JL (2000) *Catal Lett* 65:209
37. Mikael L, Niklas H, Bengt A (1998) *Appl Catal A* 166:9